

# Hot Roll Forming Analysis of Tapered Member of QP980 Steel for Lightweight Vehicles

Juanjuan Zhao, Yanzhi Guan, and Weiqiang Xue

**Abstract**—In automotive body parts, the tapered members of QP980 high-strength steel not only enable the parts to achieve ultra-high strength, but also significantly reduce the weight of the parts. However, it is different to form parts of QP980 without defects at normal temperature since QP980 has high strength and poor ductility. In view of this shortcoming, FEM software ABAQUS is used to establish the thermal-mechanical coupling finite element calculation model of QP980 high-strength steel material tapered member with local heating roll forming at different temperatures in this paper. The deformation characteristics of QP980 high strength steel in hot forming process was analyzed in terms of equivalent stress, equivalent strain, roll forming force, roll forming moment, and bending rebound. The results show that QP980 high-strength steel has good plasticity, small springback amount and good forming quality at 350 °C, and can be formed to be complex tapered members, which provides a theoretical guidance for actual QP980 sheet metal forming process.

**Index Terms**—QP980, heating forming, finite element analysis, forming quality

## I. INTRODUCTION

In the lightweight manufacturing of automobiles, the selection of high-strength steel components is regarded as one of the means to reduce fuel consumption of automobiles. In the manufacture of automotive body parts, the use of tapered members not only enables the parts to achieve the required strength, but also significantly reduces the weight of the parts. With the vigorous development of automobile light-weighting, many scholars have continuously researched and explored the roll forming technology. Data M Company is prominent in the roll forming software, which mainly studies the cold bending process of various cross-section profiles used in the automotive field, and designs and develops the first tapered roll forming prototype [1]. For the hot roll forming process and processing defects, Ozturk [2] studied the forming behavior of high-strength steel DP600

under rolling deformation with 60° bending angle. The results show that the plasticity of DP600 increases with temperature significantly improved, the amount of rebound is reduced. M. Lindgren [3] designed a rotating local heating device for roll forming for TRIP high strength steel. However, studies have shown that at normal temperature, high-strength steel has high strength, poor ductility, difficulty in forming, and defects in the formed member.

In view of these shortcomings of high-strength steel, this paper takes QP980 high-strength steel material as the research object, and combines the experimental investigation and finite element analysis method [4, 5] to study the local heating roll forming mechanism of high-strength steel. Up to now, there have been few studies on hot roll forming technology, especially the research on core technologies [6]. Roll forming is a forming process for continuously forming sheet metal. In the forming process, the multi-pass forming rolls are processed according to the forming angle of the process, and the sheet material is gradually bent laterally to obtain a metal section of a specific section [7]. In this paper, the QP980 high-strength steel material is subjected to uniaxial tensile test at 200 °C to 450 °C. Then the thermal-mechanical coupling finite element calculation model at different temperatures is established by ABAQUS software. Simulation analysis of equivalent stress, equivalent strain, roll forming force, and bending springback is carried out to study the deformation law of QP980 high strength steel during hot forming, so as to explore the optimal heating conditions to provide a theoretical basis for actual sheet metal forming [8, 9].

## II. HIGH TEMPERATURE UNIAXIAL TENSILE TEST OF QP980

### A. Materials and methods

Temperature has a great influence on the mechanical and physical properties of the materials. With the help of a tensile tester, uniaxial tensile tests at different high temperatures were carried out to obtain the accurate mechanical properties of QP980 material. In this paper, the experimental specimens were obtained by cutting the QP980 steel plate. Taking three specimens in the 0° direction, uniaxial tensile tests were performed at temperature of 200°C, 250°C, 300°C, 350°C, 400°C, and 450°C. In the uniaxial tensile test, the experimental stretching rate was 0.1 mm/min. According to the requirements of the related standard, the dimension of the uniaxial tensile test piece of the metal sheet is shown in Fig. 1.

### B. Data processing

After the high temperature uniaxial tensile test, the

Manuscript received November 16, 2019. This work was substantially supported by the National Natural Science Foundation of China (No.51775004), Beijing Natural Science Foundation (No.3164041), and Beijing Municipal Education Commission Science and Technology Foundation (No.KM201710009005).

Juanjuan Zhao is with Mechanical and Electronic Engineering Department, Shanxi Engineering Vocational College, Taiyuan Shanxi 030009, China (e-mail: zhaajuanjuan\_8@163.com).

Yanzhi Guan is with School of Mechanical and Material Engineering, North China University of Technology, Beijing 100144, China (e-mail: gyz@ncut.edu.cn).

Weiqiang Xue is with School of Mechanical and Material Engineering, North China University of Technology, Beijing 100144, China (e-mail: 1305790386@qq.com).

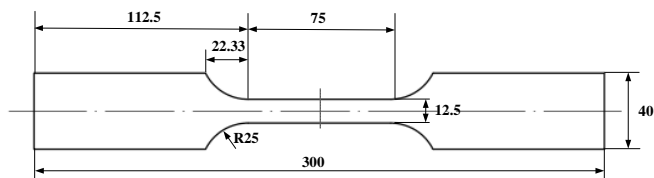


Fig. 1. Size diagram of single drawing national standard specimen

nominal stress and nominal strain of the QP980 specimen during the stretching process can be obtained. However, the true stress and strain are needed in the subsequent simulation environment. Therefore, the measured experimental data needs to be processed. According to the formula  $\sigma = \sigma_1(1 + \epsilon_1)$ ,  $\epsilon = \ln(1 + \epsilon_1)$ ,  $\sigma = F/A$ ,  $\epsilon_1 = \Delta l/l$  (where  $A$  is the cross-sectional area of the original test piece, and  $l$  is the original length of test piece,  $\Delta l$  is the change of the length of the specimen after the experiment,  $\sigma_1$  is the nominal stress,  $\epsilon_1$  is the nominal strain,  $\sigma$  is the true stress, and  $\epsilon$  is the true

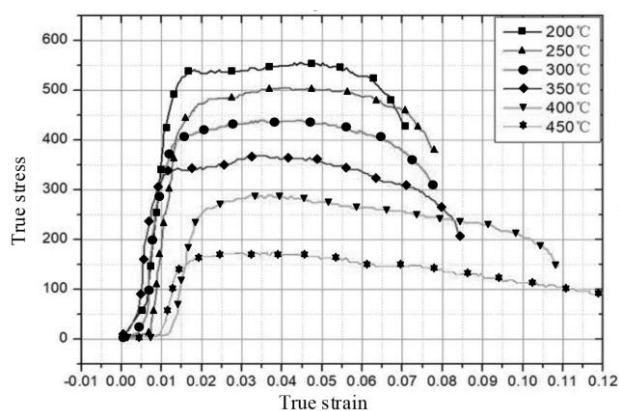


Fig. 2. Synthesis of stress-strain curves at different temperatures in 0° direction

strain). After obtaining the true stress and strain, the stress-strain curve is drawn using OriginPro software as shown in Fig. 2.

It can be seen from Fig. 2 that the tensile strength of QP980 high-strength steel is gradually decreasing as the temperature

TABLE I

QP980 PERFORMANCE PARAMETERS AT DIFFERENT TEMPERATURES

Temperature	Yield strength $\sigma_s$ /MPa	Tensile strength $\sigma_b$ /MPa	Elongation $\delta$ / %
200°C	540.04	741.32	7.6
250°C	420.66	641.36	6.9
300°C	403.67	636.52	6.4
350°C	370.2	488.30	6.7
400°C	341.28	435.59	8.6
450°C	207.53	285.56	10.8

rises. The mechanical properties of QP980 at different temperatures can be obtained from the stress-strain curve. The performance indexes are shown in Table 1.

At normal temperature, the average tensile strength of QP980 is about 1000 MPa. It can be seen from the table that the tensile strength of QP980 is greatly reduced at 200 °C to 450 °C, indicating that the temperature has a great influence on the QP980 high strength steel.

### III. FINITE ELEMENT SIMULATION AND COMPARISON OF QP980 LOCAL HEATING ROLL FORMING

In this paper, the finite element analysis software ABAQUS, which can solve large-scale nonlinear calculations, is used to simulate the hot forming of QP980 materials at different temperatures. The optimum forming temperature of the QP980 is obtained by comparative analysis of roll forming force, forming moment, stress-strain distribution, springback amount, etc. In the ABAQUS, sequential coupling stress analysis is used as follows: steady-state (or transient) thermal analysis is firstly performed to establish a thermal element model, then a thermal load is applied and solve. Then, the static structure analysis is performed, the unit type is converted into a structural unit. Finally, the thermal analysis result is applied as a load to solve the result.

#### A. Establishment of Finite Element Model for Tapered Member Roll Forming

##### a. Simplification of the finite element model

In this paper, the research is based on the tapered member unit of the fixed-die moving roll forming line. In

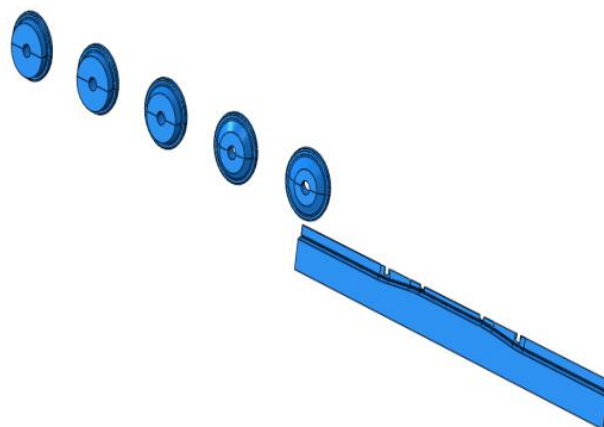


Fig. 3. Simplified model of roll bending forming part

the actual forming process, the sheet is formed by the pressure of the mold and the forming roll set. Therefore, only the mold model, the roll model and sheet metal model need to be set in the target model. Considering the deformation of the sheet, half of the entire model can be simulated when modeling. The simplified model is shown in Fig. 3.

The five passes of the model are modeled according to the actual structure. The roll forming angles are 30°, 50°, 70°, 84°, 84°. The five-stage mold in the actual structure is simplified into one whole.

##### b. Related parameter settings

The mechanical properties of the material at six temperatures have been obtained by the uniaxial tensile test of QP980 specimen, and the material properties can be set according to the tensile test results. In the actual forming process, the deformation is mainly the deformation of the rolling direction, so the data in the 0° direction is selected. The simulation analysis uses a local heating method to explore the appropriate forming

temperature, so the material properties at multiple temperatures can be set and then simulated at different temperatures.

In the simulation, the reference point and the local coordinate system are set, and the roll is set to a rotary motion. In the actual forming process, there is rolling friction and sliding friction between the sheet, the roll and the mold. For the convenience of calculation, the friction coefficient is set to a constant value of 0.15. In the actual production, the roll is hardly deformed, so the roll can be defined as a rigid body. The mold is fixed and the deformation of the mold is negligible when forming, so it can be constrained to a rigid body and the full constraint is applied thereto.

The trajectory of the roll can be discretized by the method of discretizing the trajectory to obtain some points, as long as the distance between adjacent points is small enough to simulate the true trajectory of the roll. The specific method is: applying the split point function in AutoCAD, averaging the trajectory lines according to the forming speed to obtain a plurality of points, and then

using the data extraction function to extract the coordinates of each point, and finally introducing the amplitude curve of the ABAQUS to realize the curve motion settings of the roll.

**c. Finite element model meshing**

The simplified model is imported into ABAQUS, and the mesh can be divided after the parameters are set [10, 11]. This article uses solid element analysis. Reasonable meshing not only improves the accuracy of the simulation, but also greatly reduces the running time of the computer and improves the operating efficiency. In the roll molding process, the bending deformation of the sheet material is large, and the mesh of the area should be refined. The stress of the U-shaped notch of the sheet is concentrated, therefore the mesh should be finely divided. The bottom web and side plates of the sheet are slightly deformed and can be divided by a coarse mesh [12]. For rolls and forming dies that are set to rigid bodies, quadrilateral meshes are used to mesh the objective.

*B. Analysis of heating simulation results at different temperatures*

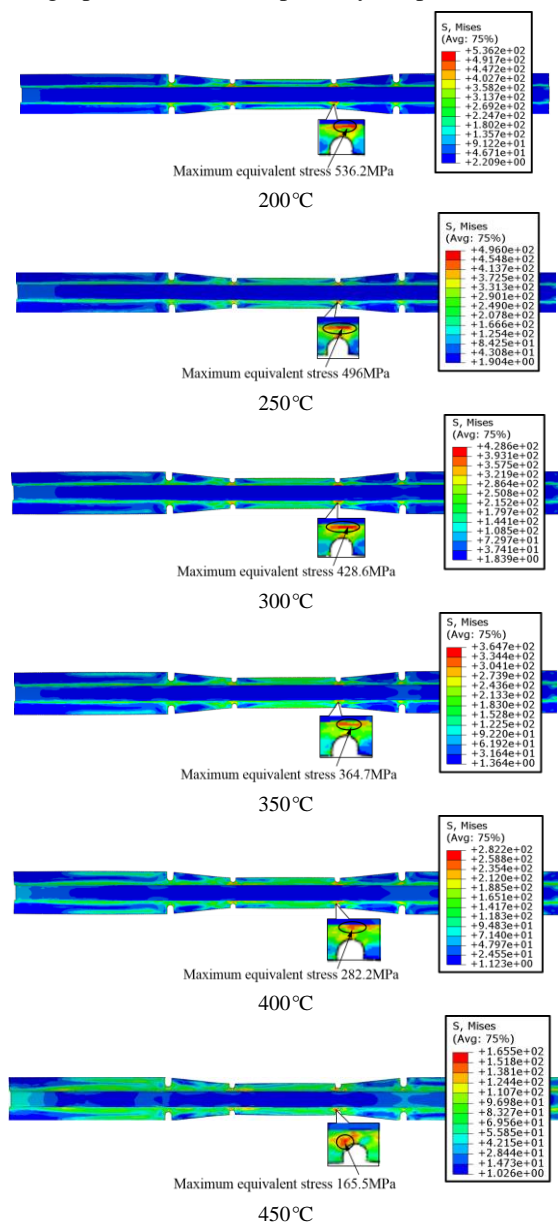


Fig. 4. Equivalent stress (Mises) diagram at different temperatures

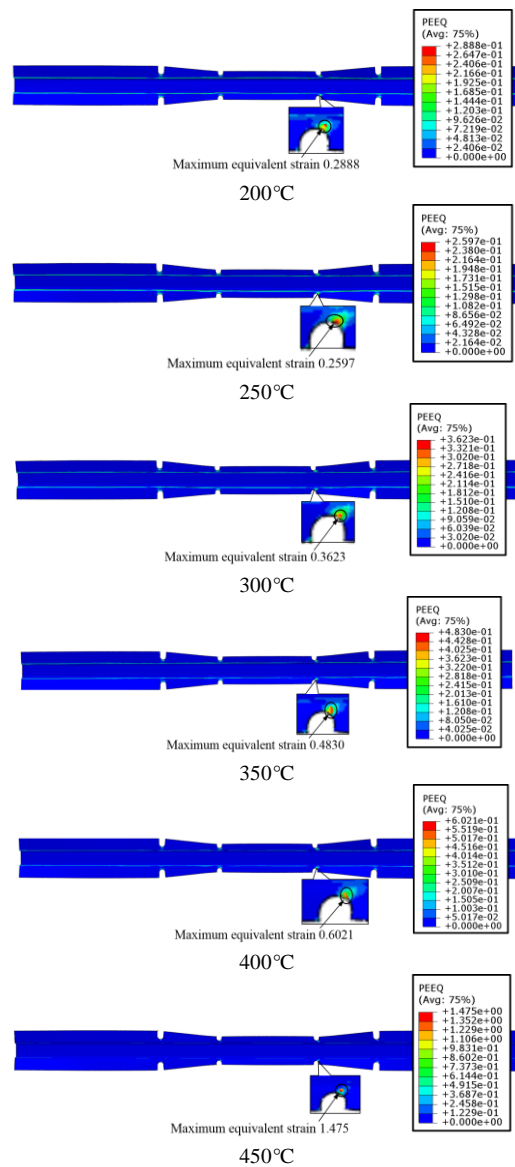


Fig. 5. Equivalent strain (PEEQ) diagram at different temperatures

**a. Stress and strain analysis**

The equivalent stress cloud diagram Mises of QP980 material at 200 °C, 250 °C, 300 °C, 350 °C, 400 °C, 450 °C is obtained, as shown in Fig.4: Stress concentration occurs in the U-shaped notch area and the corner portion where the sheet is bent, and a large residual stress occurs at the notch. At above 400 °C, the stress on each part of the sheet begins to increase. As the temperature increases, the

TABLE II

MAXIMUM EQUIVALENT STRAIN AT DIFFERENT TEMPERATURES						
Temperature /°C	200	250	300	350	400	450
Maximum average strain	0.28	0.26	0.36	0.48	0.60	1.47

maximum stress of the sheet is gradually reduced. Compared with the normal temperature, the equivalent stress decreases significantly at high temperature, and the equivalent stress is minimum at 450 °C.

Similarly, the equivalent strain cloud diagram of QP980 at temperature of 200 °C, 250 °C, 300 °C, 350 °C, 400 °C, 450 °C can be obtained, as shown in Fig.5. The results are listed in Table 2.

It can be seen from Table 2 that the plastic strain mainly occurs in the vertical plate bending zone after the forming is completed, and the maximum strain occurs in the U-shaped notch zone. The plasticity of QP980 increases under high temperature, and the strain increases obviously. The maximum equivalent plastic strain at 450 °C is about 1.47, which is obviously greater than the strain at 400 °C. This is because the elongation of the sheet is large at 450 °C, the sheet is severely deformed, and some sections are redundantly deformed, so the material is not suitable for forming at this temperature. The strain of QP980 is large at 400 °C, and the plasticity is better. From this point of view, QP980 is suitable for forming at 400 °C.

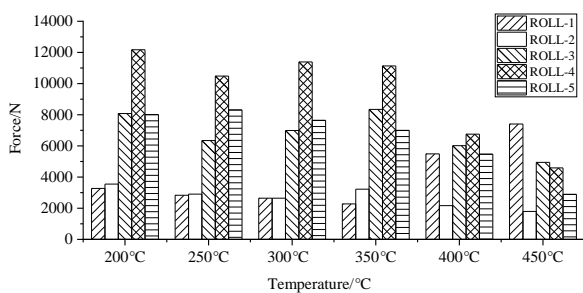


Fig. 6. Maximum forming force in Y direction of each pass at different temperatures

**b. Analysis of roll forming force results**

Since each pass roll is hardly subjected to the forming force in the Z direction [13], and the roll receives the maximum forming force in the Y direction. Therefore, the Y-direction forming force of each pass at different temperatures is extracted from multiple simulation results. The results is shown in Fig.6.

The forming force of the fourth pass of the QP980 sheet at the normal temperature is about 16KN. It can be seen from Fig.6 that the forming force of each pass is significantly reduced at high temperature. At temperatures

below 350 ° C, the forming force of the first two or three passes decreases significantly with increasing temperature. However, when the temperature is above 400 ° C, the forming force of the first pass is abnormal. This is because the plasticity of the material increases greatly when the temperature exceeds 350 ° C. It can be roughly estimated from the figure that the sheet forming effect is better between 350 ° C and 400 ° C, and the equipment requirements are lower.

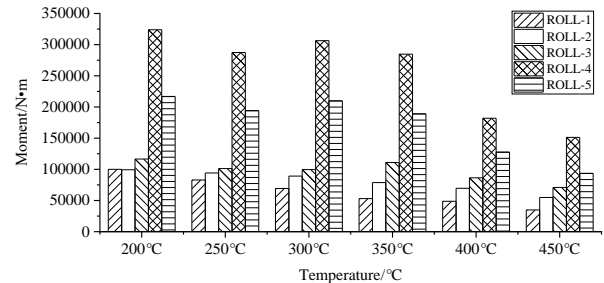


Fig. 7. Forming moment of Z-direction rolls in different passes at different temperatures

**c. Analysis of roll forming moment results**

Compared with the torque received in both directions of X and Y, the torque of the roll in the Z direction is the largest [14]. Therefore, the magnitude of the torque in the Z direction is analyzed. The same as the method of extracting the forming force, the forming moments at different temperatures obtained by the extraction are shown in Fig.7.

It can be seen from Fig.7 that as the temperature increases, the forming moment of each pass gradually decreases, and the forming moment of each pass decreases sharply at 400 °C, indicating that the plasticity of the sheet

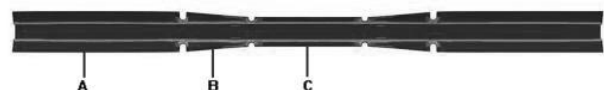


Fig. 8. Selected section position ABC of QP980 forming sheet

increases at 400 °C, which is good for forming and reduces the output requirement for the working torque of the motor.

**d. Analysis of rebound results of sheet metal parts**

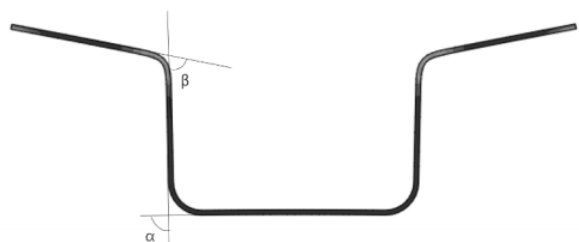


Fig. 9. The springback angle  $\alpha$  and  $\beta$  diagrams

Three different sections after sheet metal forming were extracted from the simulation results for springback analysis. The section position is shown in Fig. 8, and then the forming angles of different sections at different temperatures were extracted and analyzed.

The cross section of the shaped part at each temperature was extracted in accordance with the sectional position

TABLE III  
A COMPARISON OF SPRINGBACK ANGLE OF SECTION (UNIT: ANGLE)

Temperature	$\alpha$	$\beta$	$\Delta\alpha$	$\Delta\beta$	Object $\alpha$	Object $\beta$
200°C	89.7	79.9	0.3	4.1	90	84
250°C	89.7	81.1	0.3	2.9	90	84
300°C	89.5	81.7	0.5	2.3	90	84
350°C	89.2	82.1	0.8	1.9	90	84
400°C	89.4	83.3	0.6	0.7	90	84

TABLE IV  
COMPARISONS OF SPRINGBACK ANGLES OF SECTION B (UNIT: ANGLE)

Temperature	$\alpha$	$\beta$	$\Delta\alpha$	$\Delta\beta$	Object $\alpha$	Object $\beta$
200°C	89.1	77.9	0.9	6.1	90	84
250°C	89.2	79.6	0.8	4.4	90	84
300°C	89.3	79.9	0.7	4.1	90	84
350°C	89.3	80.4	0.7	3.6	90	84
400°C	89.5	82.7	0.5	1.3	90	84

TABLE V  
COMPARISON OF SPRINGBACK ANGLES OF SECTION C (UNITS: ANGLE)

Temperature	$\alpha$	$\beta$	$\Delta\alpha$	$\Delta\beta$	Object $\alpha$	Object $\beta$
200°C	89.6	78.8	0.4	5.2	90	84
250°C	89.6	79.5	0.4	4.5	90	84
300°C	89.6	81.2	0.4	2.8	90	84
350°C	89.6	81.1	0.4	2.8	90	84
400°C	89.5	83.9	0.5	0.1	90	84

shown in Fig. 9. In order to visually compare the forming quality of the shaped part, the forming angle of the shaped part is tabulated as shown in Tables 3 to 5 below:

In Tables 3 to 5, the target  $\alpha$  is the angle between the web of the ideal shaped part and the bottom plate,  $\alpha$  is the actual angle; the target  $\beta$  is the angle between the ideal shaped wing region and the web, and  $\beta$  is the actual angle.  $\Delta\alpha$  and  $\Delta\beta$  are the difference between the ideal forming angle of the sheet and the actual forming angle. It is known from the table that as the temperature increases, the springback of the sheet is significantly reduced. At 350 °C, the rebound angle of the three sections of the A, B, and C is small. When the temperature exceeds 350 °C, the springback amount of the sheet is minimal. However, the deformation of the sheet is large, which affects the forming quality.

Taking into account factors such as equivalent stress strain, forming force, forming moment, sheet rebound, etc., the optimum temperature is around 350 °C for QP980 sheet metal forming process.

#### IV. CONCLUSION

(1) Simplify the mechanical structure of the variable section fixed-die roller forming part, establish the model in the finite element analysis software ABAQUS, set the material properties of the sheet according to the obtained QP980 high temperature tensile test data, and mesh the model reasonably. The roll trajectory and boundary conditions are set to simulate the QP980 at different temperatures of 200 °C, 250 °C, 300 °C, 350 °C, 400 °C, 450 °C.

(2) For the QP980 forming simulation results, the appropriate forming temperature is explored from the aspects of equivalent stress, equivalent strain, roll forming force, roll forming moment, and springback analysis. Through comparative analysis, QP980 has the best forming quality at 350 °C, and can form more complex tapered members, which provides a theoretical basis for actual sheet metal forming,

and the requirements for equipment are reduced.

#### REFERENCES

- [1] Nakajima K, Miznutani W. Development of New Vertical Roll Forming Process for ERW Pipe[J]. Nippon Steel Technical Report. 1980,(15): 127-144.
- [2] Ozturk F, Toros S, Kilic S. Tensile and spring-back behavior of DP600 advanced high strength steel at warm temperatures[J]. Journal of Iron and Steel Research, International, 2009, 16(6): 41-46.
- [3] Lindgren M, Bexell U, Wikstr M L. Roll forming of partially heated cold rolled stainless steel[J]. Journal of Materials Processing Technology, 2009, 209(7): 3117-3124.
- [4] Li Hongyu, Teng Jun, Li Zuohua, Zhang Lu. Nonlinear Dynamic Analysis Efficiency by Using a GPU Parallelization[J]. Engineering Letters, 2015, 23(4): 232-238.
- [5] Yan Jinliang, Zheng Lianghong. Linear Conservative Finite Volume Element Schemes for the Gardner Equation[J]. IAENG International Journal of Applied Mathematics 2018, 45(4): 434-443.
- [6] on hot stamping[J]. Journal of 2010, 210(15): 2103-2118.
- [7] Long Jiangqi, Lan Fengchong, Chen Jiqing. New Technology of Lightweight and Steel-aluminum Hybrid Structure Car Body[J]. Journal of Mechanical Engineering, 2008, 44(6): 27-35.
- [8] Chen Gonggui, Qian Jie, Zhang Zhizhong, Sun Zhi. Multi-objective Improved Bat Algorithm for Optimizing Fuel Cost, Emission and Active Power Loss in Power System[J]. IAENG International Journal of Computer Science, 2019, 46(1): 118-133.
- [9] Patience I. Adamu, Joshua T. Jegede, Hilary I. Okagbue, and Pelumi E. Oguntunde. Shortest Path Planning Algorithm - A Particle Swarm Optimization (PSO) Approach[C] Lecture Notes in Engineering and Computer Science: Proceedings of The World Congress on Engineering, 2018, 19-24.
- [10] Hsu Yang Shang; Roberto Dalledone Machado; Joo Elias Abdalla Filho; Marcos Arndt. Numerical analysis of plane stress free vibration in severely distorted mesh by Generalized Finite Element Method [J]. European Journal of Mechanics A/Solids 62(2017)50-66.
- [11] Li Haifeng, Wu Jichuan, Liu Jianbo, Liang Yubing. Finite Element Mesh Generation and Decision Criteria of Mesh Quality[J]. China Mechanical Engineering, 2012, 23(3): 368-377.
- [12] Tan Yayun. Finite Element Analysis of Laser Assisted Heating Variable Height Roll-die Forming and Development of Laser Assisted Heating System[D]. North China University of Technology, 2016.
- [13] Li Caijun. Yield Behavior Study and Finite Element Simulation of Ultra High Strength Steel QP1180 under Local Heating[D]. North China University of Technology, 2018.
- [14] Yang Zhenfeng, Guan Yanzhi, Li Qiang, Wang Haibo. Finite element simulation of roll-die forming with variable height part[J]. Journal of Plasticity Engineering, 2018, 25(2): 137-146.